Nuclear Inst. and Methods in Physics Research, A 979 (2020) 164454

Contents lists available at ScienceDirect

Nuclear Inst. and Methods in Physics Research, A

journal homepage: www.elsevier.com/locate/nima

A charge plunger device to measure the lifetimes of excited nuclear states where transitions are dominated by internal conversion

L. Barber [a,*], J. Heery [b], D.M. Cullen [a], B.S. Nara Singh [c], R.-D. Herzberg [b], C. Müller-Gatermann [d,1], G. Beeton [c], M. Bowry [c], A. Dewald [d], T. Grahn [e], P.T. Greenlees [e], A. Illana [e], R. Julin [e], S. Juutinen [e], J.M. Keatings [c], M. Luoma [e], D. O'Donnell [c], J. Ojala [e], J. Pakarinen [e], P. Rahkila [e], P. Ruotsalainen [e], M. Sandzelius [e], J. Sarén [e], J. Sinclair [c], J.F. Smith [c], J. Sorri [f], P. Spagnoletti [c], H. Tann [b,e], J. Uusitalo [e], J. Vilhena [c], G. Zimba [e]

[a] Department of Physics & Astronomy, Schuster Building, The University of Manchester, Manchester, M13 9PL, United Kingdom
[b] Department of Physics, Oliver Lodge Laboratory, University of Liverpool, Liverpool, L69 7ZE, United Kingdom
[c] School of Computing, Engineering and Physical Sciences, University of the West of Scotland, Paisley PA1 2BE, United Kingdom
[d] Institut für Kernphysik, Universität zu Köln, D-50937 Köln, Germany
[e] Department of Physics, University of Jyvaskyla, P.O. Box 35, FI-40014 Jyvaskyla, Finland
[f] Sodankylä Geophysical Observatory, University of Oulu, Sodankylä, Finland

ARTICLE INFO

Keywords:
Charge plunger
Plunger
Nuclear-state lifetimes
RDDS
DDCM

ABSTRACT

A charge plunger device has been commissioned based on the DPUNS plunger (Taylor et al., 2013) using the in-flight mass separator MARA at the University of Jyväskylä. The ^{152}Sm(^{32}S,4n)^{180}Pt reaction was used to populate excited states in ^{180}Pt. A lifetime measurement of the 2_1^+ state was performed by applying the charge plunger technique, which relies on the detection of the charge state-distribution of recoils rather than the detection of the emitted γ rays. This state was a good candidate to test the charge plunger technique as it has a known lifetime and depopulates through a converted transition that competes strongly with γ-ray emission. The lifetime of the 2_1^+ state was measured to be 480(10) ps, which is consistent with previously reported lifetimes that relied on the standard γ-ray techniques. The charge plunger technique is a complementary approach to lifetime measurements of excited states that depopulate through both γ-ray emission and internal conversion. In cases where it is not possible to detect Doppler-shifted γ rays, for example, in heavy nuclei where internal conversion dominates, it may well be the only feasible lifetime analysis approach.

1. Introduction

The measurement of lifetimes of excited nuclear states has historically provided a useful experimental observable for assessing nuclear models. Such lifetimes allow for reduced transition rates between states to be determined, in principle allowing for the nuclear wavefunctions of the states they connect to be probed. For lifetimes of the order of a picosecond, a common experimental approach is to use a plunger device to collect recoil-distance Doppler shift (RDDS) data [1,2]. This approach relies on detecting γ-rays that are Doppler-shifted due to emission from nuclei travelling at different velocities. This difference in velocity is provided by a degrader foil situated at a variable distance from a target foil, which is referred to as a stopper foil in the case that the recoils are degraded to the extent that they are stopped. The ratio between the intensities of the γ rays emitted before and after passing through the degrader foil can then be used as a function of plunger distance to determine the lifetime of interest.

As the atomic number increases in heavy nuclei, the standard RDDS approach to lifetime measurements is hampered due to the increased probability of internal conversion events for a given energy of transition [3]. This process competes with γ-ray emission and the standard plunger approach to lifetime measurements becomes infeasible. For example, in the super-heavy nuclide ^{254}No, the yrast 2_1^+ state has an internal conversion coefficient of $\alpha = 1510(70)$ [4], which corresponds to a transition which occurs through γ-ray emission with a probability of 0.066(3)%. In cases such as this, the application of an analysis technique that relies on the detection of γ rays, such as the standard RDDS lifetime analysis approach, is not possible.

Coupled to this, the standard RDDS analysis approach to lifetime measurements requires the detection of γ rays with different Doppler

* Corresponding author.
E-mail address: liam.barber@postgrad.manchester.ac.uk (L. Barber).
[1] Present address: Physics Division, Argonne National Laboratory, Lemont, Illinois 60439, USA.

https://doi.org/10.1016/j.nima.2020.164454
Received 18 May 2020; Accepted 20 July 2020
Available online 25 July 2020

shifts that are well-resolved in energy, regardless of whether a degrader or stopper foil is used. This is usually achieved in RDDS by ensuring that there is a sufficient difference in the velocity before and after the degrader foil. A smaller difference in the recoil velocity before and after the degrader results in smaller separation in energy of the Doppler-shifted and degraded γ-ray peaks, for a given energy of γ ray transition. Therefore, it is more difficult to measure lifetimes of excited states in recoils that are produced with lower recoil velocities. It is also more difficult to detect well-resolved Doppler-shifted γ-ray peaks for transitions in which the difference in energy between the depopulating and final nuclear states is small, as the magnitude of the Doppler-shift in energy is proportional to this difference. RDDS lifetime analyses of super-heavy nuclei are therefore hampered by both a low recoil velocity and a small difference in energy between nuclear states, coupled with a high internal conversion coefficient.

An alternative method of measuring nuclear lifetimes of the order of a picosecond under these conditions, referred to as the charge plunger technique, was successfully demonstrated in 1978 [5]. This experimental approach relies on the use of a plunger device, however, the charge state of ions after internal conversion events occurring before and after a reset foil is used to measure the nuclear lifetime, rather than the Doppler-shifted energy of γ rays. The charge plunger technique is therefore applicable to lifetime measurements of excited states for which internal conversion dominates over γ-ray emission during their de-excitation or if the nuclei of interest are not produced at a sufficient velocity to allow for the detection well-resolved Doppler-shifted γ-ray peaks.

In the present work, the DPUNS plunger [6], a standard two-foil plunger, was adapted to function as a charge plunger. This device was commissioned and its ability to perform lifetime measurements through a sensitivity to the charge state of the recoils rather than the Doppler-shifted γ-rays was demonstrated. The results from this commissioning experiment, the application of the differential decay curve method (DDCM) [2,7] to charge plunger data and future applications of the device are detailed.

2. Charge plunger technique

2.1. Charge plunger device

The charge plunger technique relies on a plunger device [6], Fig. 1, that accommodates two foils, a target and a charge reset foil. The device allows for the distance between the two foils, referred to as the *plunger distance*, to be varied. A beam is incident on a target and reacts to form the nuclei of interest in the form of ions. The ions leave the target with some velocity $\boldsymbol{v_1}$ in an excited nuclear state, with a charge state that is dependent on their velocity, $\boldsymbol{v_1}$ [8]. These nuclei can then either de-excite before or after passing through the charge reset foil, which is placed downstream of the target foil. If a nucleus de-excites through an internal conversion event, there is a probability that the nucleus will emit Auger electrons. This leaves the nucleus in a highly positive charged state due to the loss of electrons. An internal conversion event and subsequent Auger cascade that occurs after the ions have passed through the charge reset foil will result in the ions leaving the plunger device in a highly charged state. Alternatively, if such an event occurs before passing through the charge reset foil, the ions will gain electrons on passing through the charge reset foil. The ions will then leave the plunger in a lower charge state, due to the acceptance of electrons from the charge reset foil. The time scale that Auger emission occurs is of the order of femtoseconds [9], while the time of flight between the plunger foils is of the order of a picosecond. This ensures that the time period over which Auger cascade occurs has no dependence on the resulting charge-state distribution of the recoils, as an Auger cascade will occur physically close to position of the internal conversion event, relative to the plunger distance. De-excitation though γ-ray emission does not result in an Auger cascade, and as a result such recoils remain in a low charge state regardless of whether the de-excitation occurs before or after the charge reset foil.

There are numerous methods that can be deployed in order to gain sensitivity to the charge state of the ions. For example, in Ref. [5] a tabletop-sized magnetic deflector and photographic plate were used, whereas in the present work the mass-separator MARA [10,11] was used in conjunction with a position sensitive Multi-Wire-Proportional Counter (MWPC) and a double sided silicon strip detector (DSSSD) at its focal plane [11]. With sensitivity to the number of ions detected downstream of the plunger device in the high charge state, I_{high}, and the low charge state, I_{low}, the ratio between these two quantities can be found as a function of the plunger distance, x. Knowledge of this ratio, as well as the internal conversion coefficient of the transition of interest, can be used to determine the fraction of nuclei that decayed before and after passing through the charge reset foil, and therefore, the lifetime of the state of interest can be deduced.

In order for an ion to be detected in the high charge state, it must have de-excited after passing through the charge reset foil (subsequently referred to as *after reset*, a.r.) and also undergo an internal conversion process, i.e.,

$$I_{\text{high}} = I_{\text{a.r.}} p_{\text{int}}, \tag{1}$$

where p_{int} is the probability that the transition of interest will depopulate through internal conversion,

$$p_{\text{int}} = \frac{\alpha}{(1+\alpha)}, \tag{2}$$

with an internal conversion coefficient α. These expressions assume that there is a single transition with a significant rate of internal conversion that has a lifetime, τ, such that $x \sim \tau v$.

Similarly, in order for an event to be detected in the low charge state, it can either de-excitation before the charge reset foil (b.r.), or de-excitation after passing the charge reset foil through any channel other than internal conversion, i.e.,

$$I_{\text{low}} = I_{\text{b.r.}} + I_{\text{a.r.}}(1 - p_{\text{int}}). \tag{3}$$

The number of events occurring before and after the reset foil are then given by,

$$I_{\text{a.r.}}(x) = I_{\text{high}}(x)\frac{(1+\alpha)}{\alpha} \tag{4a}$$

$$I_{\text{b.r.}}(x) = I_{\text{low}}(x) - \frac{I_{\text{high}}(x)}{\alpha}, \tag{4b}$$

where the dependence of the expressions on the plunger distance, x, has been highlighted.

Through variation of the plunger distance, x, the ratio between $I_{\text{b.r.}}$ and $I_{\text{a.r.}}$ can be determined as a function of x. This allows for the lifetime of the state of interest to be determined through application of the differential decay curve method (DDCM) [2,7], or through directly fitting the Bateman equations to the data.

2.2. DDCM with a charge plunger device

The differential decay curve method (DDCM) [2,7] is an analysis technique that is commonly applied to RDDS data collected using a standard plunger. The analysis technique can also be applied to data collected with a charge plunger once the number of events occurring before the reset foil (b.r.) and after the reset foil (a.r.) have been calculated through Eq. (4). For an experiment in which the recoil events of interest can be linked to a specific feeding transition, such as through the application of a γ-ray coincidence gate, the lifetime of the state of interest, τ_i, which is fed by a transition B and depopulates through a transition A is given by

$$\tau_i = \frac{1}{|\boldsymbol{v_1}|}\frac{I_{\{B_{\text{b.r.}},A_{\text{a.r.}}\}}(t)}{\frac{\text{d}}{\text{d}x}\left(I_{\{B_{\text{b.r.}},A_{\text{b.r.}}\}}(t)\right)}, \tag{5}$$

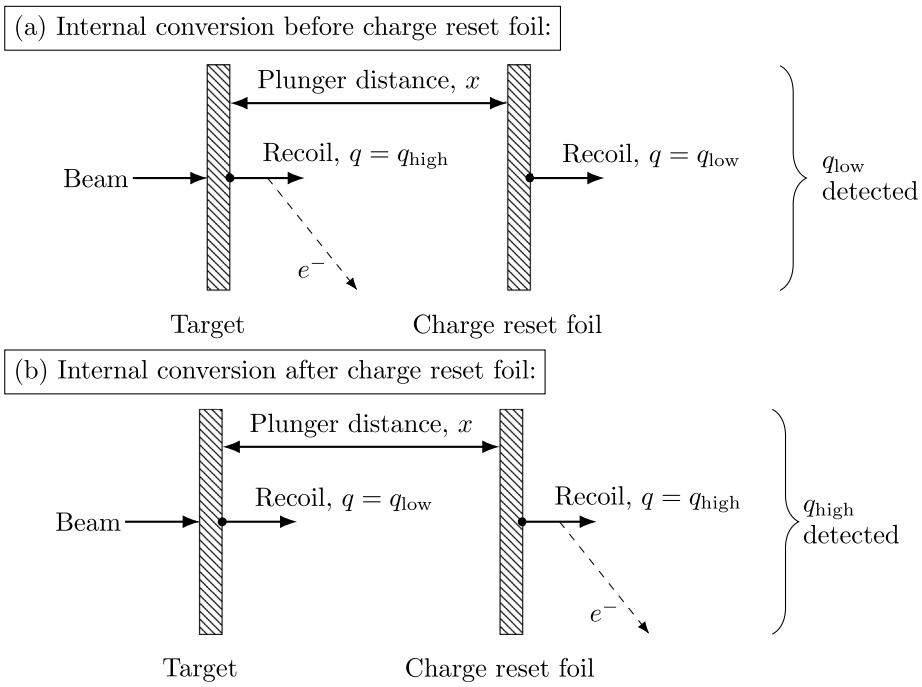

Fig. 1. A schematic of a charge plunger device, consisting of a target foil and a charge reset foil separated by a distance x. The charge state of the nuclide of interest is shown for internal conversion events and subsequent Auger cascades that occur before (a) or after (b) the charge reset foil. De-excitation though γ-ray emission does not result in an Auger cascade, and as a result such recoils remain in a low charge state regardless of whether the de-excitation occurs before or after the charge reset foil.

where the notation $I_{\{X,Y\}}$ is used to represent the number of detected transitions Y when a coincidence gate is applied to the transition X.

Application of the DDCM has several advantages over simply fitting the Bateman equation to the data. For example, problems that occur due to unobserved side feeding can be removed through applying DDCM with a γ-ray coincidence analysis. This allows for events that populate the state of interest only through a specific transition to be considered. Additionally, a DDCM analysis is independent of the absolute plunger distance, and relies only on the difference between plunger distances. This results in the analysis being independent of the offset of the foils, the separation between the foils when they reach electrical contact. This is a source of systematic uncertainty in determining absolute plunger distances. Finally, the lifetimes of the nuclear states that directly or indirectly feed the state of interest do not need to be assumed in order to perform a DDCM analysis in which a γ-ray coincidence gate is applied. This is not the case for applying the Bateman equations directly.

There is also an additional advantage in the application of DDCM over the Bateman equations specifically in the analysis of charge plunger data. The method used to determine τ through the application of DDCM and the software Napatau [12] are independent of the internal conversion coefficient, α, of the state of interest, providing $I_{\text{a.r.}}$ and $I_{\text{b.r.}}$ are normalised by their sum at each plunger distance. This is significant as the internal conversion coefficients are often from theoretical calculations tabulated in databases such as BrIcc [13], rather than from experimental measurements. While in principle it is possible to determine such coefficients experimentally, this introduces an additional source of uncertainty in the final lifetime measurement. A lifetime analysis that is independent of α therefore allows for measurements that are model independent while minimising their uncertainty.

The fitting procedure carried out by Napatau in order to determine an experimental lifetime minimises the function

$$\chi^2 = \sum_{i=0}^{N}\left(\frac{I_{\text{b.r.}} - f\left(a_0, a_1, a_2; t_i\right)}{\sigma\left(I_{\text{b.r.}}\right)}\right)^2 + \left(\frac{I_{\text{a.r.}} - t\frac{\mathrm{d}f(a_0,a_1,a_2;t_i)}{\mathrm{d}t}}{\sigma\left(I_{\text{a.r.}}\right)}\right)^2 \quad (6)$$

where the function f is a second-order polynomial with coefficients (a_0, a_1, a_2), σ is the standard deviation and t is the lifetime that is varied to find the minimum χ^2. The value of t which minimises Eq. (6) for a given i is the experimental lifetime, τ_i, obtained at the distance x_i. The summation is carried out over the total N number of measured distances.

This fitting procedure of Eq. (6) results in a measured lifetime that has no significant dependence on the internal conversion coefficient α if the quantities $I_{\text{b.r.,a.r.}}$ are normalised by their sum at each plunger distance. For example, in the lifetime analysis presented in this paper, allowing α to range from $\alpha = 1$ to $\alpha \to \infty$ changed the measured lifetime by $\sim 0.01\sigma$, where σ is the uncertainty on the lifetime. This is not the case for the approach of fitting Bateman equations to the data, in which the α dependence of $I_{\text{a.r.}}, I_{\text{b.r.}}$ has a significant effect on the measured lifetime.

3. Commissioning experiment

3.1. Experimental procedure

The charge plunger device was commissioned through a measurement of the lifetime of the 2_1^+ yrast state in ^{180}Pt. This state has both a known lifetime and a significant rate of internal conversion, $\alpha_{2_1^+} = 0.922(9)$ [14], allowing the charge plunger technique to be applied. The ^{180}Pt nuclei of interest were produced through the fusion–evaporation reaction ^{152}Sm(^{32}S, $4n$)^{180}Pt at an beam energy of 165 MeV in the laboratory frame. The energy of the beam was optimised to give a maximum production cross section for the channel of interest relative to the other isobars produced, according to PACE4 [15]. The target consisted of 1.0 mg cm^{-2} ^{152}Sm with 1.5 mg cm^{-2} $^{\text{nat.}}$Ta backing.

The two-foil plunger DPUNS [6] was adapted to function as a charge plunger by replacing the degrader foil with a $^{\text{nat.}}$Ni charge reset foil of thickness 0.29 mg cm^{-2}. This allowed for the recoiling ions to exchange electrons with atoms in the charge reset foil on passing through it, without being significantly slowed down. The feedback system [6] of DPUNS ensured that the two plunger foils remained at a constant separation during the experiment. Throughout the experiment, a pulsed

signal of 10 V was applied to the target foil and the induced voltage on the charge reset foil was recorded in order to provide a measure of the capacitance between the foils to the feedback system.

The $A \sim 180$ isobars of interest are separated from the beam through use of the recoil separator, MARA [10,11]. This recoil separator consists of three quadrupole magnets, an electric dipole magnet and a magnetic dipole magnet. A position-sensitive MWPC and a DSSSD implantation detector were located at the focal plane of MARA, which were surrounded by germanium clover detectors. This setup allowed for the recoil energy, velocity, position and incoming angle of the recoil to be measured [10]. The time of flight of the recoils between the MWPC and DSSD detectors is also measured. These observables allow for the recoil events of interest to be differentiated from the scattered beam. Recoiling ions with a given reference energy, E_{ref}, and reference charge state, q_{ref}, could be selected to allow for a given energy and charge of recoils to pass along the optical axis and be detected at the centre of the focal plane by using the appropriate MARA parameter settings. This allowed for the mass to charge ratio, m/q, of the recoiling ions to be measured. Given the mass of the recoiling ions, MARA has a sensitivity to the charge state-distribution of the recoils, which was necessary to perform a lifetime analysis with the charge plunger device.

Prompt γ rays emitted from the excited recoils were also detected at the target position using the Jurogam 3 array [16]. This detector array consists of 15 Eurogam high purity Ge (HPGe) phase 1 detectors and 24 HPGe clover detectors. These detectors were arranged into four rings with a combined efficiency of 5.2% at 1.3 MeV. The detection of prompt γ rays provided a method of normalising the number of recoil events at the focal plane of MARA by the rate of recoil production at the target. This allowed for fluctuations in the intensity of the beam and the length of time of data collection to be corrected for across the range of plunger distances and charge states that data were collected for. Although not necessary for the implementation of the charge plunger technique, the detection of γ-rays allowed for recoil events detected at MARA to be tagged by the specific γ-ray transitions, through use of the triggerless data readout (TDR) data acquisition system [17]. The high selectivity of events made it possible to perform a DDCM lifetime analysis according to Eq. (5) using a charge plunger device.

3.2. The ideal case of ^{180}Pt

A measurement of the lifetime of the 2_1^+ yrast state in ^{180}Pt is an ideal case to commission the charge plunger device for several reasons. Firstly, there are measured values of $\tau_{2_1^+}$ within the literature; $\tau_{2_1^+} = 540(50)$ ps [18] from an RDDS measurement, and both $\tau_{2_1^+} = 420(20)$ ps [19] and $\tau_{2_1^+} = 420(30)$ ps [19] through applying fast-timing techniques, respectively. These allow for a measurement of $\tau_{2_1^+}$ through the charge plunger technique to be verified. There is also significant internal conversion of the $2_1^+ \rightarrow 0_1^+$ transition, $\alpha_{2_1^+} = 0.922(9)$, which is necessary for the application of the charge plunger technique. The properties of the $4_1^+ \rightarrow 2_1^+$ direct feeder transition to the 2_1^+ state also makes commissioning the charge plunger through the measurement of $\tau_{2_1^+}$ possible. There is a strong direct feeding transition to the 2_1^+ state from the 4_1^+ state, allowing for a DDCM analysis to be applied and remove the effects of side feeding. Additionally, the magnitude of the internal conversion of the 4_1^+ state is much less than that of the 2_1^+ state. This ensures that a γ-ray coincidence gate can be set on the feeding transition, which both allows for the DDCM analysis of Eq. (5) and excludes any conversion events due to the depopulation of the 4_1^+ state. Furthermore, the lifetime of the 4_1^+ state and those higher in excitation energy are much shorter than the lifetime of the 2_1^+ state. This ensures that any conversion events that do occur earlier in time than the depopulation of the 2_1^+ state do not affect the charge state-distribution within the region of sensitivity for the 2_1^+ lifetime measurement. Here, the region of sensitivity for a given state refers to the range of plunger distances for which the fraction of decays occurring before and after the charge reset foil changes with the plunger distance, i.e. the range of plunger distances, x, such that $x \sim |\boldsymbol{v_1}|\tau$.

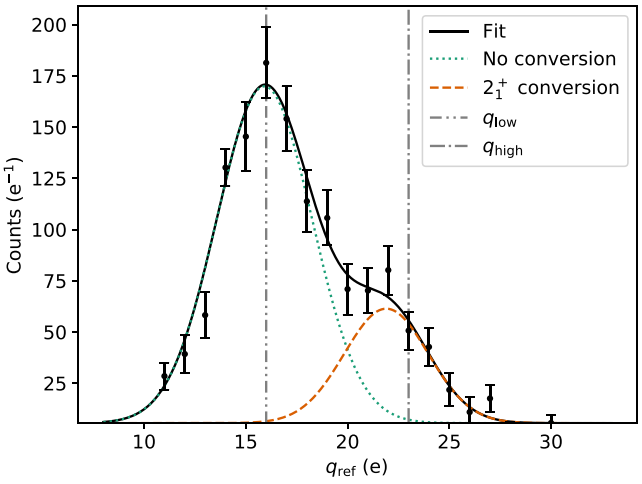

Fig. 2. The number of recoil events detected at the focal plane of MARA as a function of the reference charge, q_{ref}. This was recorded for a fixed $E_{\text{ref}} = 20$ MeV and plunger distance $x = 1707(2)$ μm. The distribution of charge states is well described by two normal distributions. These two peaks correspond to internal conversion events occurring after the reset foil and any other events. The number of events at two points in this distribution, $q_{\text{low,high}}$ were recorded for each plunger distance, which were converted into the number of events in each distribution.

4. Results of commissioning experiment

4.1. Charge state-distribution

In order to determine the properties of the ^{180}Pt recoil charge state-distribution, the recoil detection rate was measured as a function of the reference charge, q_{ref}. The resulting recoil detection rate is plotted as a function of q_{ref} for a fixed $E_{\text{ref}} = 20$ MeV in Fig. 2. The charge state-distribution is well fitted by two normal distributions with centroids $\mu = 15.9(3), 21.9(8)$ e and widths $\sigma = 2.3(2), 2.0(5)$ e for the low and the high charge states, respectively. These parameters were free parameters in the fit, and so were experimentally deduced for this reaction. The high charge state corresponds to events in which internal conversion occurs after the foil, while the low charge state correspond any other events.

Characterising the charge state-distribution is necessary in order to extract the proportion of events which were detected in the high and low charge states. This is because only the number of events at two points in the charge state distribution, q_{high} and q_{low}, were measured as a function of plunger distance during the experiment, rather than the full distribution. These two reference charges are highlighted within the charge state-distribution of Fig. 2. In general, these values are not proportional to the number of events in each charge state-distribution, due to the finite widths of the distributions characterising each charge state, and a choice of $q_{\text{high,low}}$ that differs from the centroid of each distribution. The widths and centroids of the charge state-distributions were measured from the data shown in Fig. 2. This allowed for the amplitudes and integrals of the high and low charge state-distributions to be calculated, given the recoil rate at q_{high} and q_{low}, for each plunger distance, x.

Additionally, measurement of the charge state-distribution verified that there were no significant internal conversion events occurring after the reset foil from the de-excitation of excited states that are higher in energy than the 2_1^+ state in ^{180}Pt. Excited states that have a significant rate of internal conversion and a similar lifetime to the state of interest would create a third charge state-distribution. It would then be necessary to separate the contribution to the overall charge state-distributions from the de-excitation of each excited state. This could be done through the application of γ-ray coincidence gates.

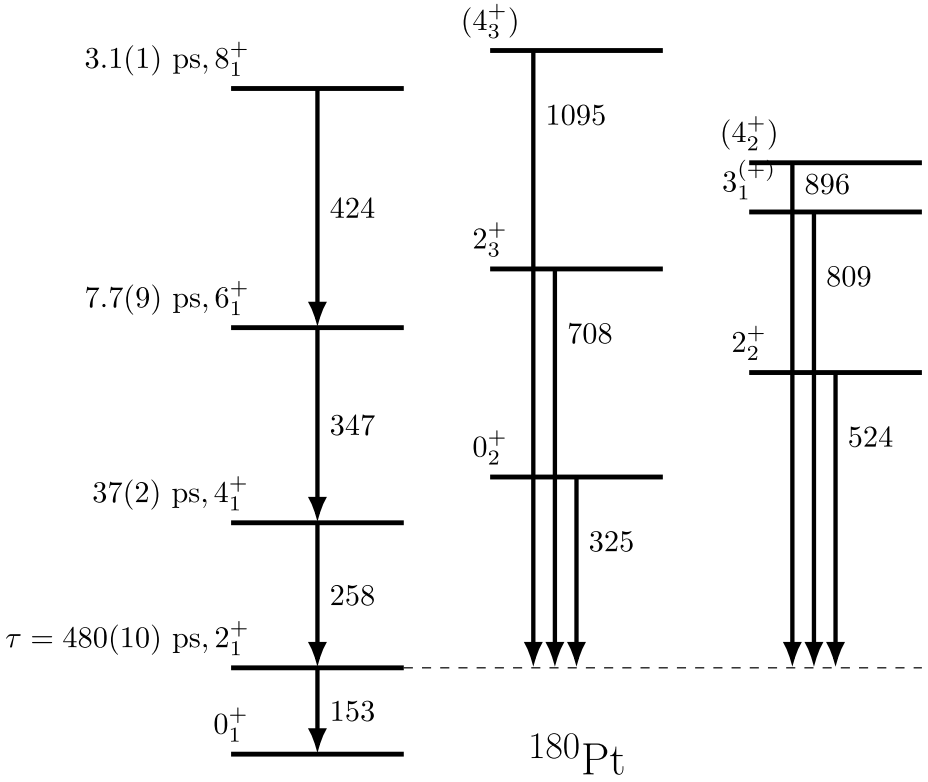

Fig. 3. A partial level scheme showing some of the low-lying states in ^{180}Pt [14]. The energies of a selection of the transitions feeding the yrast 2^+ state of interest are also shown in kilo-electron-volts, with measured lifetimes from taken from Ref. [19], with the exception of $\tau_{2_1^+}$ which was measured in the present work.

4.2. Lifetime DDCM analysis

The lifetime of the 2_1^+ state in ^{180}Pt was measured following the charge plunger technique outlined in Section 2. An energy level scheme for the low-lying states in ^{180}Pt is given in Fig. 3.

Data were collected at seven plunger distances ranging from x = 63.1(3) μm to x = 4988.6(3) μm. The choice of plunger distances ranged from $x \ll \tau_{2_1^+}|\boldsymbol{v_1}|$ to $x \gg \tau_{2_1^+}|\boldsymbol{v_1}|$, where $\tau_{2_1^+}|\boldsymbol{v_1}| \sim 2500$ μm. This range of plunger distances allowed for the region of sensitivity of the 2_1^+ lifetime to be probed. At each plunger distance, MARA was used to select two charge states of the recoils, referred to as the low charge state, $q_{\text{ref}} = q_{\text{low}} = 16e$, and the high charge state, $q_{\text{ref}} = q_{\text{high}} = 24e$. The values of the two reference charges were chosen such that the rate of recoil detection for each charge state was maximised, while ensuring that there was no significant contribution from the other charge state.

A two-dimensional gate was set on the energy of recoils versus time of flight between the MWPC and implantation detector at the focal plane of MARA. This gate is shown in Fig. 4. This allowed for a separation of the ^{180}Pt recoils of interest from the scattered beam. The γ-ray spectrum of recoils selected through use of this gate is shown in Fig. 5a, with the γ-ray peaks of interest highlighted. There are a significant number of events from the de-excitation of excited states in ^{179}Pt when the recoil gate is applied alone.

A γ-ray coincidence gate was also set on the $4_1^+ \rightarrow 2_1^+$ transition of ^{180}Pt, as well as a background gate. This allowed for the effects of side feeding on the measured lifetime to be removed, as is standard in a DDCM analysis. Application of these gates also removed the ^{179}Pt contaminant and other $A = 180$ isobars. The resulting γ-ray spectrum for events in coincidence with a $4_1^+ \rightarrow 2_1^+$ γ-ray event and a recoil event at the focal plane of MARA is shown in Fig. 5b.

The m/q of recoil events at the focal plane of MARA in coincidence with both the recoil and γ-ray coincidence gates were used to perform the lifetime analysis. These m/q distributions are shown in Fig. 6 for a range of plunger distances. The range of m/q values that could be

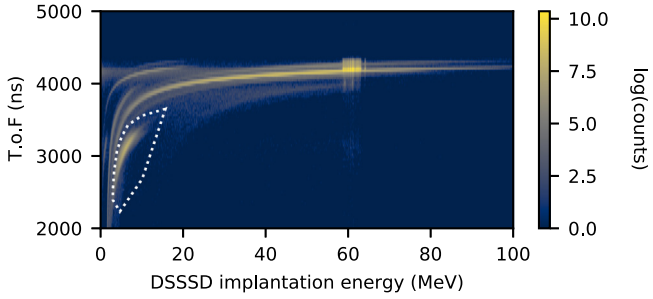

Fig. 4. The recoil gate applied to the recoil time of flight (T.o.F.) versus energy plot. This allowed for the recoils to be selected from the scattered beam. The recoils are primarily ^{180}Pt, as well as ^{179}Pt and other $A = 180$ isobars.

detected simultaneously was limited by the size of the DSSD at the focal plane of MARA, and as a result it was not possible to have sensitivity to the entirety of the charge state-distribution at once at the focal plane. Instead, events were detected at one of two reference charges, referred to as the high, q_{high}, and the low, q_{low}, charge states. The integral of the central peak in each m/q spectrum at a given reference charge was measured for the range of plunger distances, x, for both the high and the low charge states. The central peak was used as this corresponded to events occurring along the optical axis of MARA, and so were the events for which both the charge and energy distributions of recoils centred on $q = q_{\text{ref}}$ and $E = E_{\text{ref}}$. The limits that were used to determine these integrals are highlighted in Fig. 6. The resulting integrals were normalised by the total number of events in coincidence with the $4_1^+ \rightarrow 2_1^+$ γ-ray transition of ^{152}Sm, excited through Coulomb excitation. Alternative normalisation constants were also obtained through events in coincidence with γ-ray transitions from ^{180}Pt which resulted in a consistent analysis. The rate of recoil detection at the focal plane of MARA does not reflect the rate of production of

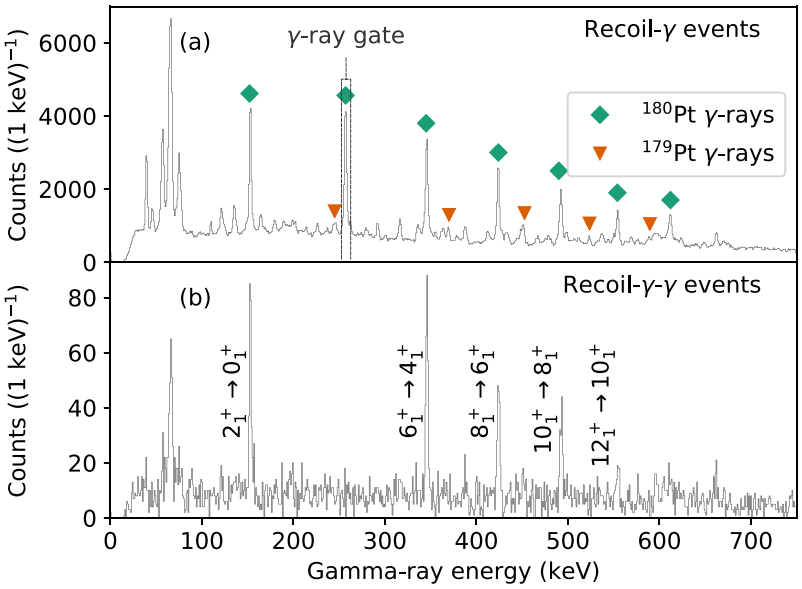

Fig. 5. The γ-ray events detected by Jurogam 3, consisting of 15 Eurogam high purity Ge (HPGe) phase 1 detectors and 24 HPGe clover detectors, after applying different coincidence gates. (a) γ-ray events in coincidence with the recoil gate of Fig. 4. Gamma-rays in coincidence with the $4^+_1 \rightarrow 2^+_1$ transition of ^{180}Pt and those originating from the contaminant ^{179}Pt are highlighted. (b) γ-ray events in coincidence with both the recoil gate and γ-rays from the coincidence gate highlighted in (a). The γ-ray peaks are labelled by their initial and final states.

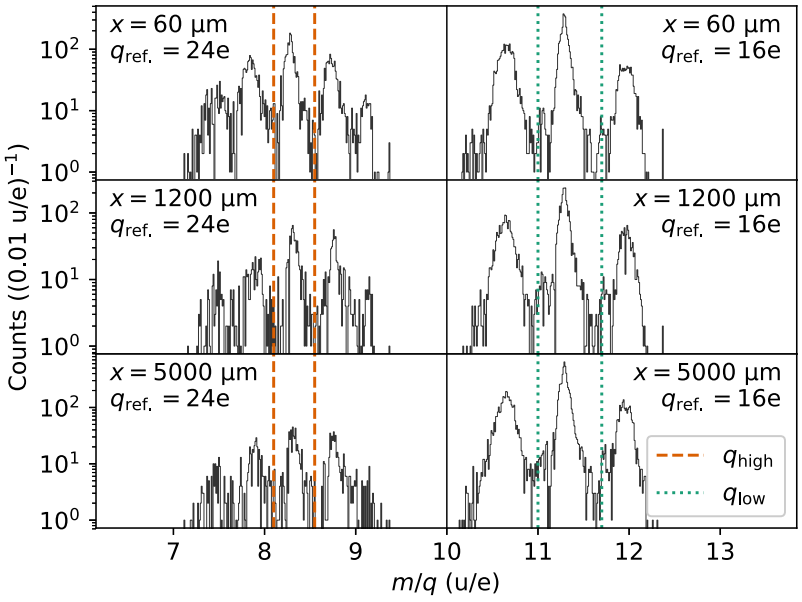

Fig. 6. The mass per unit charge, m/q, distribution of recoils for a selection of plunger distances, for a fixed reference energy of 20 MeV and both $q_{\text{ref}} = 16\,\text{e}, 24\,\text{e}$. The limits on the integral of the high and low charge states are shown, which covers the central peak in the DSSD. This peak was chosen as it corresponds to ions which travel down the optical axis of MARA, and so the distribution of energy and charge for these ions correspond to q_{ref} and E_{ref}. The ratio of low to high charge state events increases with plunger distance, as is expected.

^{180}Pt, as MARA selects a subset of recoils with distributions centred on particular q_{ref} and E_{ref}. As a result, raw Jurogam 3 events were used to obtain the normalisation, with no application of coincidence gates from events at the MARA focal plane. The resulting normalised I_{high} and I_{low} were applied to Eqs. (4a) and (4b) in order to determine the fraction of decays occurring before and after the reset foil. These are plotted in Fig. 7c as a function of plunger distance, x.

The DDCM expression given by Eq. (5) relies on the detection of events that are in coincidence feeding transitions that occur before the reset foil, $B_{\text{b.r.}}$. In a standard DDCM analysis of RDDS data, this requirement is met by only gating on the fully shifted component of the direct feeding γ-ray transition. However, as the charge plunger has a charge reset foil in place of a degrader foil, there is a negligible difference between the velocity of the recoils before and after the charge reset foil, $\Delta v \sim 0.002c$. As a result, it is not possible to apply a γ-ray coincidence gate on a specific transition occurring before the reset foil, as both the transitions occurring before and after the reset foil appear as a single unresolved γ-ray peak when detected. It is therefore necessary to only perform the DDCM analysis using plunger distances that satisfy $x \gg \tau_{4+}|\boldsymbol{v}_1|$, to ensure that there is not a significant number of $4^+_1 \rightarrow 2^+_1$ decays occurring after the reset foil, as Eq. (4) assume a single transition with significant internal conversion.

This approach was verified by applying the unresolved Doppler-shifted components method (UDCM) [20] to the unresolved $4^+_1 \rightarrow 2^+_1$ γ-ray transition. The measured shift in energy of the unresolved $4^+_1 \rightarrow 2^+_1$ γ-ray peak could then be used to calculate the fraction of these

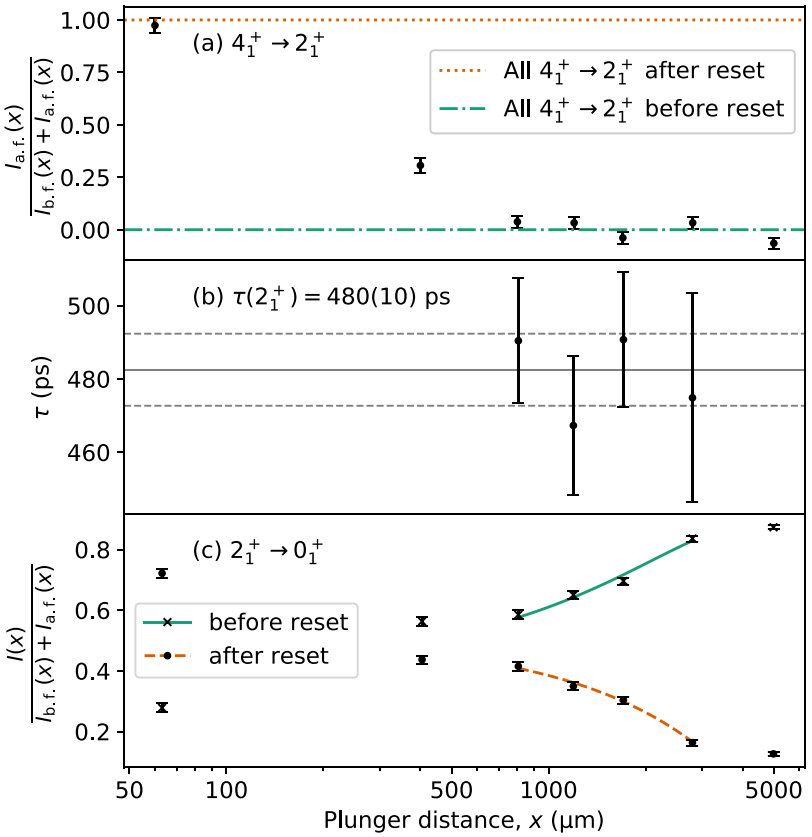

Fig. 7. (a) The fraction of $4_1^+ \rightarrow 2_1^+$ transitions occurring after the charge reset foil, as a function of the plunger distance, x. This was used to justify the application of the DDCM expression given by Eq. (5) for $x > 400$ μm. (b) The lifetime plot for the 2_1^+ state in ^{180}Pt. (c) The fraction of the events occurring before and after the reset detector are plotted as a function of plunger distance. The second order polynomial that was fitted to the data in order to perform a DDCM lifetime analysis is shown.

transitions that occurred before and after the reset foil as a function of plunger distance, x. This dependence is plotted in Fig. 7(a), with the points at which all of the decays occur before or after the reset foil highlighted. There is a significant fraction of the $4_1^+ \rightarrow 2_1^+$ decays occurring after the reset foil for the two smallest plunger distances, $x = 60$ μm and $x = 400$ μm. However, the fraction of $4_1^+ \rightarrow 2_1^+$ decays occurring after the reset foil for $x > 400$ μm are all consistent with zero. This was used to justify the omission of the data collected at $x = 60$ μm and $x = 400$ μm when performing the DDCM analysis for the determination of $\tau_{2_1^+}$, as the variation of I_{high} and I_{low} at these plunger distances will have a dependence on $\tau_{4_1^+}$.

A second order polynomial was fitted piecewise to $I_{\text{b.r.}}$ and its differential multiplied by $\tau|\boldsymbol{v_1}|$ was fitted to $I_{\text{a.r.}}$. The programme NAPATAU was used in order to calculate the lifetime at each plunger distance, through Eq. (5). The lifetimes obtained for the range of plunger distances considered are shown in Fig. 7b. These were combined through a weighted mean to form the experimental measurement of $\tau_{2_1^+} = 480(10)$ ps. The uncertainty presented on this measurement includes contributions from both the random uncertainties associated with the finite number of events recorded and also the systematic uncertainties arising due to the fitting procedure. The present measurement of $\tau_{2_1^+}$ obtained using the charge plunger technique is consistent with the previously reported measurements of this lifetime, $\tau_{2_1^+} = 540(50)$ ps [18], $\tau_{2_1^+} = 420(20)$ ps [19] and $\tau_{2_1^+} = 420(30)$ ps [19], to within 1.2σ, 2.7σ and 1.9σ, respectively. The measurement of $\tau_{2_1^+}$ through application of the charge plunger technique is also consistent with the weighted mean of the previous measurements, $\tau_{2_1^+} = 430(20)$ ps to within 2.2σ.

The adapted plunger device described in this work will allow for the charge plunger technique to be applied at the Accelerator Laboratory at the University of Jyväskylä. This technique will be of use in the measurement of excited nuclear states that have a high rate of internal conversion. Specifically, it would be more efficient to perform the charge plunger technique if the rate of internal conversion between two nuclear states $i \rightarrow j$ is higher than the strongest γ-ray transition depopulating the state i, $i \rightarrow k$, assuming an equal overall detection efficiency for events in each case. Additionally, if the velocity of the recoil of interest is not sufficiently large for the standard RDDS analysis technique to be applied then the charge plunger technique would be feasible for any $\alpha_{ij} > 0$, where α_{ij} is the internal conversion coefficient between states $i \rightarrow j$.

5. Conclusion

The standard two-foil plunger DPUNS has been adapted to perform a lifetime analysis using the charge plunger technique. The lifetime of the 2_1^+ yrast state in ^{180}Pt was measured to be 480(10) ps through a commissioning experiment at the Accelerator Laboratory at the University of Jyväskylä in order to verify the performance of the adapted device. This result is consistent with the previously reported values. This device will allow for measurements of the lifetimes of excited nuclear states in nuclei with high rates of internal conversion, such as super-heavy nuclei, that would not have been accessible with standard γ-ray lifetime techniques.

Declaration of competing interest

The authors declare that they have no known competing financial interests or personal relationships that could have appeared to influence the work reported in this paper.

Acknowledgements

We gratefully acknowledge the support of accelerator staff and the students at the JYFL accelerator facility of the University of Jyväskylä. This work was supported by the EU 7th Framework Programme, Integrating Activities Transnational Access, Project No. 262010 ENSAR and support from GAMMAPOOL for the loan of the JUROGAM 3 detectors. L.B. and D.M.C. acknowledge support of the Science and Technology Facilities Council, UK, Grant Nos. ST/L005794/1 and ST/P004423/1. C.M-G. and A.D. were supported by the Deutsche Forschungs Gemeinschaft (DFG), Germany under contract number DE 1516/5-1.

References

[1] T.K. Alexander, A. Bell, A target chamber for recoil-distance lifetime measurements, Nucl. Instrum. Methods 81 (1) (1970) 22–26, http://dx.doi.org/10.1016/0029-554X(70)90604-X, URL http://www.sciencedirect.com/science/article/pii/0029554X7090604X.

[2] A. Dewald, S. Harissopulos, P.v. Brentano, The differential plunger and the differential decay curve method for the analysis of recoil distance Doppler-shift data, Z. Phys. A 334 (2) (1989) 163–175, http://dx.doi.org/10.1007/BF01294217, URL https://link.springer.com/article/10.1007/BF01294217.

[3] O. Dragoun, M. Rysavý, O. Dragoun, A. Spalek, Internal conversion coefficients for superheavy elements, J. Phys. G: Nucl. Part. Phys. 26 (10) (2000) 1461–1466, http://dx.doi.org/10.1088/0954-3899/26/10/302.

[4] B. Singh, Nuclear data sheets for $A = 254$, Nucl. Data Sheets 156 (2019) 1–69, http://dx.doi.org/10.1016/j.nds.2019.02.003, URL http://www.sciencedirect.com/science/article/pii/S009037521930016X.

[5] G. Ulfert, D. Habs, V. Metag, H.J. Specht, Lifetime measurements of nuclear levels with the charge plunger technique, Nucl. Instrum. Methods 148 (2) (1978) 369–379, http://dx.doi.org/10.1016/0029-554X(70)90191-6, URL http://www.sciencedirect.com/science/article/pii/0029554X70901916.

[6] M.J. Taylor, D.M. Cullen, A.J. Smith, A. McFarlane, V. Twist, G.A. Alharshan, M.G. Procter, T. Braunroth, A. Dewald, E. Ellinger, C. Fransen, P.A. Butler, M. Scheck, D.T. Joss, B. Saygi, C.G. McPeake, T. Grahn, P.T. Greenlees, U. Jakobsson, P. Jones, R. Julin, S. Juutinen, S. Ketelhut, M. Leino, P. Nieminen, J. Pakarinen, P. Peura, P. Rahkila, P. Ruotsalainen, M. Sandzelius, J. Sarén, C. Scholey, J. Sorri, S. Stolze, J. Uusitalo, A new differentially pumped plunger device to measure excited-state lifetimes in proton emitting nuclei, Nucl. Instrum. Methods Phys. Res. A 707 (Suppl. C) (2013) 143–148, http://dx.doi.org/10.1016/j.nima.2012.12.120, URL http://www.sciencedirect.com/science/article/pii/S0168900213000028.

[7] A. Dewald, O. Moller, P. Petkov, Developing the recoil distance Doppler-shift technique towards a versatile tool for lifetime measurements of excited nuclear states, Prog. Part. Nucl. Phys. 67 (3) (2012) 786–839, http://dx.doi.org/10.1016/j.ppnp.2012.03.003, URL http://www.sciencedirect.com/science/article/pii/S0146641012000713.

[8] G. Schiwietz, P.L. Grande, Improved charge-state formulas, in: Twelfth International Conference of Ion Beam Modification of Materials, Nucl. Instrum. Methods Phys. Res. B 175–177 (2001) 125–131, http://dx.doi.org/10.1016/S0168-583X(00)00583-8, URL http://www.sciencedirect.com/science/article/pii/S0168583X00005838.

[9] S.-K. Son, R. Santra, Monte Carlo calculation of ion, electron, and photon spectra of xenon atoms in x-ray free-electron laser pulses, Phys. Rev. A 85 (6) (2012) 063415, http://dx.doi.org/10.1103/PhysRevA.85.063415.

[10] J. Sarén, J. Uusitalo, M. Leino, P.T. Greenlees, U. Jakobsson, P. Jones, R. Julin, S. Juutinen, S. Ketelhut, M. Nyman, P. Peura, P. Rahkila, C. Scholey, J. Sorri, The new vacuum-mode recoil separator MARA at JYFL, in: Proceedings of the XVth International Conference on Electromagnetic Isotope Separators and Techniques Related to their Applications, Nucl. Instrum. Methods Phys. Res. B 266 (19) (2008) 4196–4200, http://dx.doi.org/10.1016/j.nimb.2008.05.027, URL http://www.sciencedirect.com/science/article/pii/S0168583X08007040.

[11] J. Uusitalo, J. Sarén, J. Partanen, J. Hilton, Mass analyzing recoil apparatus, MARA, Acta Phys. Polon. B 50 (3) (2019) 319, http://dx.doi.org/10.5506/APhysPolB.50.319, URL http://www.actaphys.uj.edu.pl/findarticle?series=Reg&vol=50&page=319.

[12] B. Saha, Program NAPATAU, Institute for Nuclear Physics, Cologne, unpublished.

[13] T. Kibédi, T.W. Burrows, M.B. Trzhaskovskaya, P.M. Davidson, C.W. Nestor Jr., Evaluation of theoretical conversion coefficients using BrIcc, Nucl. Instrum. Methods Phys. Res. A 589 (2) (2008) 202–229, http://dx.doi.org/10.1016/j.nima.2008.02.051, URL http://www.sciencedirect.com/science/article/pii/S0168900208002520.

[14] E.A. McCutchan, Nuclear data sheets for A = 180, Nucl. Data Sheets 126 (2015) 151–372, http://dx.doi.org/10.1016/j.nds.2015.05.002, URL http://www.sciencedirect.com/science/article/pii/S0090375215000137.

[15] O.B. Tarasov, D. Bazin, Development of the program LISE: application to fusion–evaporation, in: 14th International Conference on Electromagnetic Isotope Separators and Techniques Related to their Applications, Nucl. Instrum. Methods Phys. Res. B 204 (2003) 174–178, http://dx.doi.org/10.1016/S0168-583X(02)01917-1, URL http://www.sciencedirect.com/science/article/pii/S0168583X02019171.

[16] J. Pakarinen, J. Ojala, P. Ruotsalainen, H. Tann, H. Badran, T. Calverley, J. Hilton, T. Grahn, P.T. Greenlees, M. Hytönen, A. Illana, A. Kauppinen, M. Luoma, P. Papadakis, J. Partanen, K. Porras, M. Puskala, P. Rahkila, K. Ranttila, J. Sarén, M. Sandzelius, S. Szwec, J. Tuunanen, J. Uusitalo, G. Zimba, The Jurogam 3 Spectrometer, The European Physical Journal A 56 (5) (2020) 149, http://dx.doi.org/10.1140/epja/s10050-020-00144-6, https://doi.org/10.1140/epja/s10050-020-00144-6.

[17] I.H. Lazarus, E.E. Appelbe, P.A. Butler, P.j. Coleman-Smith, J.R. Cresswell, S.J. Freeman, R.D. Herzberg, I. Hibbert, D.T. Joss, S.C. Letts, R.D. Page, V.F.E. Pucknell, P.H. Regan, J. Sampson, J. Simpson, J. Thornhill, R. Wadsworth, The GREAT triggerless total data readout method, IEEE Trans. Nucl. Sci. 48 (3) (2001) 567–569, http://dx.doi.org/10.1109/23.940120.

[18] M.J.A. De Voigt, R. Kaczarowski, H.J. Riezebos, R.F. Noorman, J.C. Bacelar, M.A. Deleplanque, R.M. Diamond, F.S. Stephens, J. Sauvage, B. Roussière, Collective and quasiparticle excitations in 180Pt, Nuclear Phys. A 507 (2) (1990) 472–496, http://dx.doi.org/10.1016/0375-9474(90)90304-5, URL http://www.sciencedirect.com/science/article/pii/0375947490903045.

[19] C. Müller-Gatermann, A. Dewald, C. Fransen, T. Braunroth, J. Jolie, J. Litzinger, J.M. Régis, F. von Spee, N. Warr, K.O. Zell, T. Grahn, P.T. Greenlees, K. Hauschild, U. Jakobsson, R. Julin, S. Juutinen, S. Ketelhut, P. Nieminen, M. Nyman, P. Peura, P. Rahkila, P. Ruotsalainen, M. Sandzelius, J. Sarén, C. Scholey, J. Sorri, S. Stolze, J. Uusitalo, P. Petkov, Low-lying electromagnetic transition strengths in ^{180}Pt, Phys. Rev. C 97 (2) (2018) 024336, http://dx.doi.org/10.1103/PhysRevC.97.024336, URL https://link.aps.org/doi/10.1103/PhysRevC.97.024336.

[20] L. Barber, D.M. Cullen, M.M. Giles, B.S. Nara Singh, M.J. Mallaburn, M. Beckers, A. Blazhev, T. Braunroth, A. Dewald, C. Fransen, A. Goldkuhle, J. Jolie, F. Mammes, C. Müller-Gatermann, D. Wölk, K.O. Zell, Performing the differential decay curve method on γ-ray transitions with unresolved doppler-shifted components, Nucl. Instrum. Methods Phys. Res. A 950 (2020) 162965, http://dx.doi.org/10.1016/j.nima.2019.162965, URL http://www.sciencedirect.com/science/article/pii/S0168900219313567.